J. Astrophys. Astr. (2008) **29,** 29–39

Global Solar Dynamo Models: Simulations and Predictions

Mausumi Dikpati* & Peter A. Gilman**
High Altitude Observatory, NCAR, 3080 Center Green, Boulder CO 80301, USA.
**e-mail: dikpati@hao.ucar.edu*
***e-mail: gilman@hao.ucar.edu*

Abstract. Flux-transport type solar dynamos have achieved considerable success in correctly simulating many solar cycle features, and are now being used for prediction of solar cycle timing and amplitude. We first define flux-transport dynamos and demonstrate how they work. The essential added ingredient in this class of models is meridional circulation, which governs the dynamo period and also plays a crucial role in determining the Sun's memory about its past magnetic fields. We show that flux-transport dynamo models can explain many key features of solar cycles. Then we show that a predictive tool can be built from this class of dynamo that can be used to predict mean solar cycle features by assimilating magnetic field data from previous cycles.

Key words. Sun—magnetic fields: solar cycle—dynamo—prediction.

1. Introduction and philosophical approach

In the current era of extensive use of the high atmosphere and neighboring interplanetary medium by man, solar cycle predictions have considerable practical value. Starting with solar cycle 22 (1986–96), NASA and other Federal Agencies concerned with the effects of solar activity on human activity have convened cycle prediction panels to assess all predictions and methods used, and give their best judgment on the amplitude and other properties of the next cycle. For cycles 22 and 23, prediction methods were primarily statistical rather than dynamical. That is, no physical laws were integrated forward in time, as is done for meteorological and climate predictions. On the verge of the onset of solar cycle 24, the first such 'dynamo based' cycle prediction, which involves integrating forward in time a form of Faraday's law of electromagnetic theory, has now been made (Dikpati *et al.* 2006; Dikpati & Gilman 2006).

Given the complexity of the physics in the interior of the Sun, how is such a prediction possible? Any such model must be able to simulate the important features of a 'typical' solar cycle (Dikpati *et al.* 2004), such as the 'butterfly diagram', and the phase relation in time between toroidal (sunspot) fields and poloidal (polar) fields. It must do this with differential rotation and meridional circulation that are close to that observed in the Sun. In other words, the dynamo model must be 'calibrated' with solar observations. This process also constrains the choice of more poorly known physical parameters, such as the magnetic diffusivity. Once calibrated, the model can be used to simulate and predict

departures from the typical cycle, caused by variations in various input data, such as observed magnetic fields from previous times. We and others have therefore focussed attention on a class of dynamo model that has enough physics in it to be calibratible with global solar observations, while at the same time being integratible using modest computing resources. This class of dynamo is the 'flux transport' dynamo, so named (Wang & Sheeley 1991) because of the inclusion of meridional circulation as well as differential rotation in the induction equation. Such models generally parameterize key turbulent processes occurring on scales smaller than the resolution of the model, such as the turbulent transport of magnetic flux captured by a turbulent magnetic diffusivity, and the turbulent lifting and twisting of magnetic field lines represented by one or more 'α-effects'. These models also do not include the buoyant eruption of toroidal flux tubes, turbulent diamagnetic effects and Alfvén wave effects. The success of such a model in simulating and predicting solar cycles can only be judged by studying the ouput from it, by comparing it to the appropriate solar observations. Figure 1 shows a sequence of schematic diagrams that depict qualitatively the succession of processes contained in a flux-transport dynamo solution that leads to cyclic magnetic fields of the correct dominant symmetry about the equator. The historical evolution of large-scale solar dynamo models, starting from the first model by Parker (1955) was reviewed by Dikpati (2004b). Here we focus primarily on flux-transport dynamo mechanism and the predictive tool development from it.

2. Mathematical formulation

We start from the axisymmetric, mean-field dynamo equations and write them as:

$$\frac{\partial A}{\partial t} + \frac{1}{r\sin\theta}(\mathbf{u}\cdot\nabla)(r\sin\theta A) = \eta\left(\nabla^2 - \frac{1}{r^2\sin^2\theta}\right)A + S(r,\theta,B_\phi) + \frac{\alpha B_\phi}{1+(B_\phi/B_0)^2}, \quad (1)$$

$$\frac{\partial B_\phi}{\partial t} + \frac{1}{r}\left[\frac{\partial}{\partial r}(ru_rB_\phi) + \frac{\partial}{\partial\theta}(u_\theta B_\phi)\right] = r\sin\theta(\mathbf{B}_p\cdot\nabla)\Omega - \hat{\mathbf{e}}_\phi\cdot[\nabla\eta\times\nabla\times B_\phi\hat{\mathbf{e}}_\phi] + \eta\left(\nabla^2 - \frac{1}{r^2\sin^2\theta}\right)B_\phi, \quad (2)$$

in which $B_\phi(r,\theta,t)\,\hat{\mathbf{e}}_\phi$ and $\nabla\times A(r,\theta,t)\,\hat{\mathbf{e}}_\phi$ respectively represent the toroidal and poloidal fields.

In equation (1), $S(r,\theta,B_\phi)$ represents the production of new poloidal field from the decay of tilted, bipolar active regions at the surface, and α is an α-effect that arises from global instabilities in the overshoot tachocline (see Dikpati & Gilman 2001 for details). In equation (2), $\Omega(r,\theta,t)$ is the specified differential rotation, parameterized from helioseismology, and in both equations $\mathbf{u} = u_r\,\hat{\mathbf{e}}_r + u_\theta\,\hat{\mathbf{e}}_\theta$ is the specified meridional circulation. In equation (1), α now is an α-effect that arises from instabilities in the overshoot tachocline near the bottom of the domain. The details of the tachocline α-effect we have used, such as its latitudinal profile, are given in Dikpati & Gilman (2001). Both the surface poloidal source and the α-effect near the bottom of the domain are 'quenched' above a certain field strength, so that the

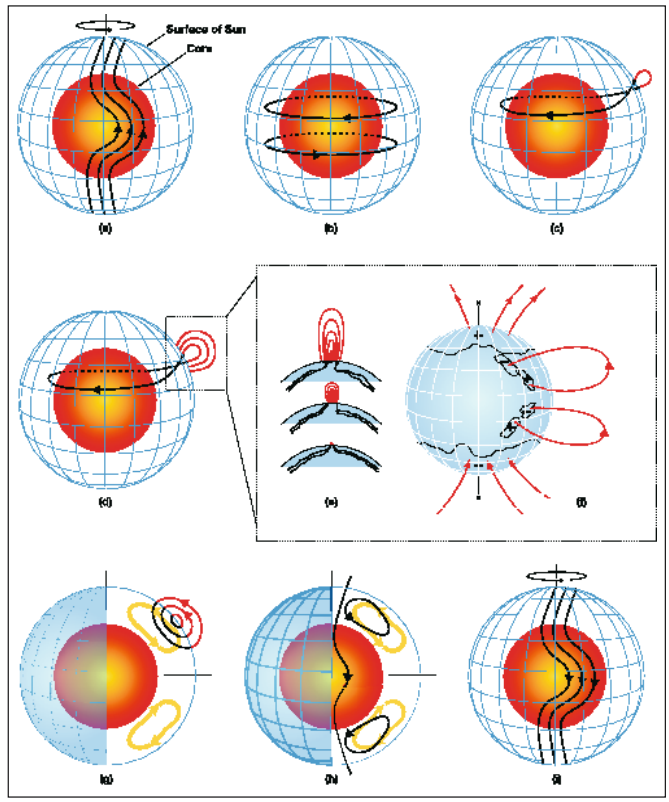

Figure 1. Schematic of solar flux-transport dynamo processes. Red inner sphere represents the Sun's radiative core and blue mesh the solar surface. In between is the solar convection zone where dynamo resides. **(a)** Shearing of poloidal field by the Sun's differential rotation near convection zone bottom. The Sun rotates faster at the equator than the pole. **(b)** Toroidal field produced due to this shearing by differential rotation. **(c)** When toroidal field is strong enough, buoyant loops rise to the surface, twisting as they rise due to rotational influence. Sunspots (two black dots) are formed from these loops. **(d, e, f)** Additional flux emerges **(d, e)** and spreads **(f)** in latitude and longitude from decaying spots (as described in Fig. 5 of Babcock 1961). **(g)** Meridional flow (yellow circulation with arrows) carries surface magnetic flux poleward, causing polar fields to reverse. **(h)** Some of this flux is then transported downward to the bottom and towards the equator. These poloidal fields have sign opposite to those at the beginning of the sequence, in frame (a). **(i)** This reversed poloidal flux is then sheared again near the bottom by the differential rotation to produce the new toroidal field opposite in sign to that shown in (b).

solutions do not grow without bound. This is the only nonlinearity in the system. The boundary conditions we apply are: the toroidal field is zero on all boundaries, while the poloidal field is fitted to a potential field above the top boundary. $A = 0$ at the poles is required by axisymmetry. $A = 0$ at the bottom boundary ($r = 0.6$R) keeps the field out of the deep interior, and in the case of a single hemisphere calculation, $B_\phi = 0$; $\partial A/\partial\theta = 0$ at the equator to ensure the antisymmetric magnetic field solutions. In full sphere calculations, the equatorial boundary conditions are omitted.

3. Major results since 1999

3.1 *What determines the period of the solar activity cycle?*

A principal result of Dikpati and Charbonneau (1999) was to show that in flux transport dynamos, the dynamo period is approximately inversely proportional to the meridional flow speed. Agreement between the model cycle period and that of the Sun requires an equatorward return flow of a few m/s near the base of the convection zone. The cycle period in flux-transport dynamos is rather insensitive to the amplitude of the differential rotation, α effects, or the diffusivity, in contrast to that in the so-called interface dynamos (Parker 1993) and classical α-ω dynamo (Stix 1973).

3.2 *What determines the phase relation between the tachocline toroidal field and the surface radial field?*

Wang *et al.* (1989) first showed, using a one-dimensional flux-transport model applied to the Sun's surface, that advective-diffusive transport of the Sun's weak magnetic flux arising from the decay of active regions can explain quantitatively the poleward drifts of these flux and the polar reversal during sunspot maximum. This was confirmed by simulations from a complementary 2D flux-transport model by Dikpati (1996) for a meridional cut in the Sun's convective envelope. In a detailed Babcock-Leighton flux-transport dynamo calculation with solar-like differential rotation, Dikpati and Charbonneau (1999) showed that this phase relation is a natural consequence of the meridional flow of observed amplitude on the Sun. The key to getting the correct phase relation between the peak in the toroidal fields and sunspots, and the surface poloidal fields, particularly the polar field reversals is having the primary creation of toroidal fields occurring near $r = 0.7$R, while the poloidal flux is created at the surface and transported towards the pole by surface processes.

3.3 *What causes the solar dynamo to operate in a mode predominantly antisymmetric about the equator, as exemplified by Hale's polarity laws?*

Babcock-Leighton type advection-dominated flux-transport dynamos cannot produce solar-like antisymmetric magnetic fields about the equator. By doing full spherical shell simulations without imposing equatorial symmetry conditions, Dikpati & Gilman (2001) showed that the combination of a meridional flow towards the equator at the bottom of the convection zone, together with an α-effect there, favors the antisymmetric mode.

The physical reason why an advection-dominated Babcock-Leighton dynamo does not relax to an antisymmetric mode is that the poloidal fields generated at the surface diffuse away in the course of their long traversal to meet with their opposite-hemisphere counterparts and to form an extended equatorial dipole, which is necessary for producing antisymmetric toroidal fields. In contrast, poloidal fields produced by a tachocline α-effect are swept towards the equator quickly by the equatorward meridional flow there, and hence can couple the two hemispheres by antisymmetric magnetic fields.

3.4 *Can flux-transport dynamos explain features of global solar magnetism specific to a particular solar cycle?*

Dikpati *et al.* (2004) was the first to apply a flux-transport dynamo to explain specific features of a particular solar cycle, that of cycle 23. The model was first calibrated against an average solar cycle, and then initialized with magnetic data from cycle 22. They found that the 1.5-year delay in polar field reversal in cycle 23 compared to an average cycle was primarily due to the weaker surface poloidal field sources in cycle 23 compared to 22. When transported to the poles by the meridional circulation, these weaker sources took longer to cancel out the polar field created during cycle 22. These weaker sources also caused the post-reversal polar field of cycle 23 to be weaker than in cycle 22, and take longer to build up. Dikpati *et al.* (2004) also explained that the $\sim$ 50% slow-down in the meridional flow-speed during 1996–2003 (Haber *et al.* 2002; Basu & Antia 2003) together with the N-S asymmetry in this flow, caused the North Pole reverse $\sim$ 1 year before the South Pole.

In response to Choudhuri and collaborators' "million-dollar question" raised in various emails spread over the world (including in the Diamond Jubilee conference at PRL) about the correctness of Dikpati *et al.* (2004) results, we (Dikpati & Gilman 2007) recently published the steps for building such a model (see Fig. 2) and re-confirmed the results of the calibrated dynamo of Dikpati *et al.* (2004).

3.5 *Can the so-called interface dynamos calibrate well to the Sun?*

Parker (1993) defined and applied the first interface dynamo to the Sun. In its simplest form this dynamo contains a radial differential rotation characteristic of the solar tachocline, together with an α-effect just above the tachocline. The magnetic diffusivity is taken to be much smaller in the tachocline than above it. Parker showed that it is capable of producing large amplitude toroidal fields in the tachocline due to the low diffusivity, where they can be stored long enough to reach the strength needed to be the source of sunspots seen in middle and low latitudes.

But does such a solution calibrate well with solar observations? For example, does it produce a butterfly diagram from toroidal field near $r = 0.7$R and surface radial field that agrees well with that of the real Sun? Also, Garaud (1999) showed that the skin-depth of cyclically reversing poloidal fields near the base of the convection zone can be severely limited by the rapidly declining magnetic diffusivity there. What if conditions are such that these poloidal fields can not penetrate the tachocline enough to be sheared by the radial rotation gradient there? In that case, a pure interface dynamo might fail completely. Dikpati *et al.* (2005) showed in the absence of tachocline radial shear participating in the dynamo process, a latitudinal differential rotation can provide the necessary Ω-effect to drive an oscillation in an interface dynamo, but it alone cannot produce the latitudinal migration. They concluded that a flux-transport dynamo driven by both the Babcock-Leighton and interface/bottom α-effects is a robust dynamo for the Sun.

3.6 *Can the currently operating solar dynamo be a significant source of toroidal flux in the solar interior below the convection zone?*

One of the remaining mysteries concerning radiative stellar interiors is whether they contain magnetic fields, and if so, what kind and of what magnitude. Two concepts are

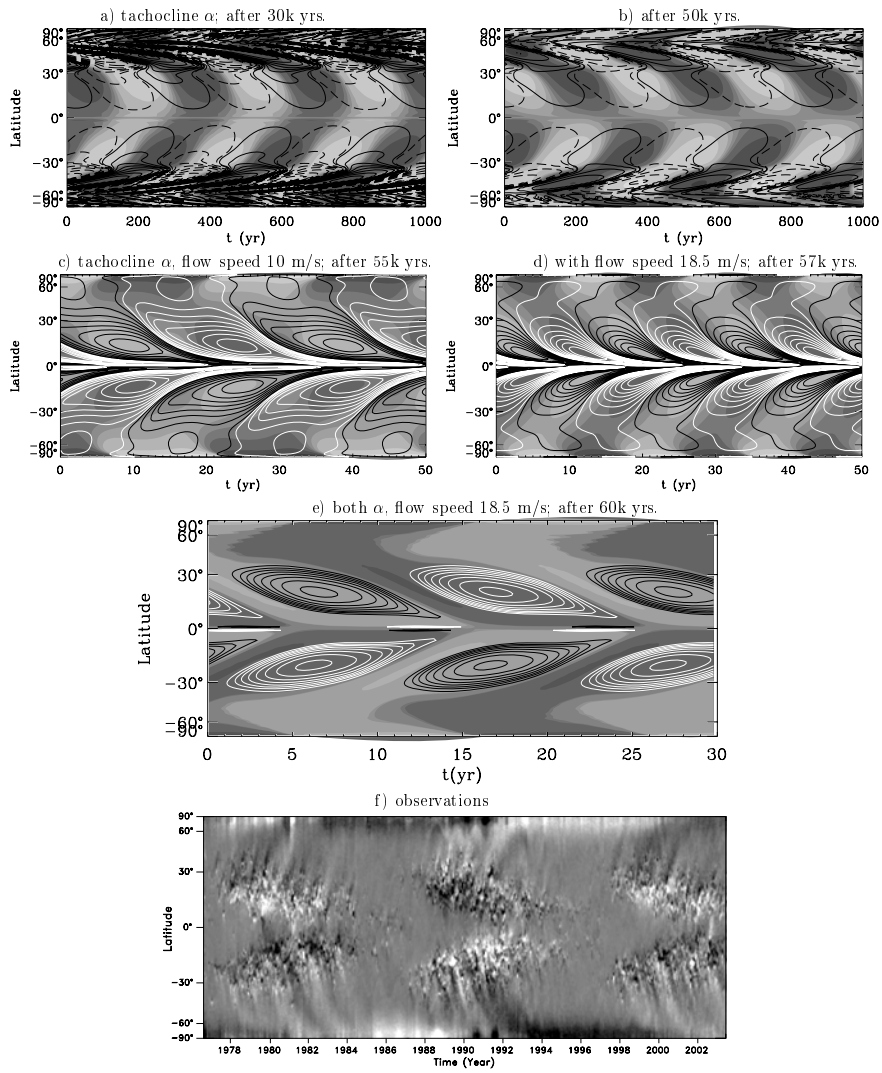

Figure 2. **(a, b)**: Butterfly diagrams for $B_r|_R$ (gray shades) and $B_\phi|_{ov}$ (contours) after 30 k (less evolved), 50 k years, with differential rotation, tachocline α-effect but no meridional circulation. **(c, d)**: Butterfly diagrams with meridional circulation ($u_{\rm mc}$) added; **(c)** for maximum $u_{\rm mc} = 10\,{\rm ms}^{-1}$ after another 5 k years' run; **(d)** maximum $u_{\rm mc} = 18.5\,{\rm ms}^{-1}$, after additional 2 k years' run. Here the cycle period is governed by meridional circulation. **(e)**: Butterfly diagram with Babcock-Leighton α-effect added, after 3 k years' run (though 50 years is enough). $B_\phi|_{ov}$ and $B_r|_R$ patterns in latitude show very good agreement with surface observations **(f)** (from Fig. 8 of DDGAW).

that such fields are primordial (Cowling 1945; Wrubel 1952) or that they are remnant fields from extinct dynamos (Schüssler 1975; Parker 1981). Mestel and Weiss (1987) suggested that convection zone dynamos with cycles fluctuating in amplitude could create net interior fields. Dikpati *et al.* (2006) show that flux-transport dynamos producing very regular cycles in the convection zone can create substantial non-reversing

toroidal fields in the outer part of the stellar interior, provided there is an α-effect near the bottom of the convection zone. Their results should apply to stellar interiors generally.

3.7 *Can the timing of the end of a cycle and the onset of the next one be predicted?*

Since for flux-transport dynamos the period is set primarily by the amplitude of the meridional flow, if that flow changes from one cycle to the next or within a given cycle, the length of that cycle will be affected. Starting from Dikpati *et al.*'s (2004) calibrated dynamo, Dikpati (2004a) performed a series of numerical experiments starting from cycle 22 and allowing for different meridional flow amplitudes during cycle 23. The resulting time trace of the induced toroidal field in the model tachocline for the different meridional flows is shown in Fig. 3. Here we see that, compared to a meridional flow set by the average cycle period for cycles 12–22 (10.75 yrs), if the meridional flow decelerates during 1996–2003 and then remains low, the onset of cycle 24 will be delayed by about 12 months, leading to new cycle spots exceeding the old cycle spots in early 2008. If the meridional flow instead accelerates after 2003, some of the delay can be made up, resulting in a net delay of about 6 months. This prediction of late onset of cycle 24 is now supported by a variety of observational evidence. For example, the observational butterfly diagram from NASA shown in Fig. 3(c) shows clearly that we have not yet (at the start of 2007) reached minimum. There is still significant cycle 23 activity in the Southern Hemisphere. In addition, the corona is not yet in minimum

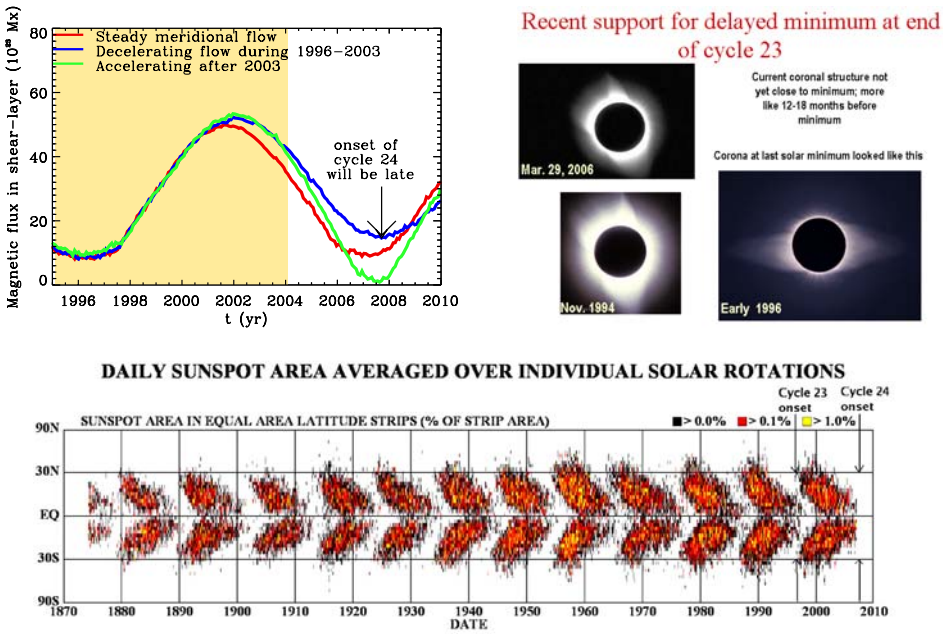

Figure 3. **(a)** Time trace of integrated toroidal flux in bottom shear layer for simulations beginning in 1995 with 3 different meridional flow variations with time; **(b)** Coronal images at eclipse, showing 2006 corona not at minimum phase; **(c)** Observed butterfly diagram from David Hathaway's website (http:solarscience.msfc.nasa.govimagesbfly.gif).

phase. This we can see in Fig. 3(b), which shows that the corona at total eclipse of March 29, 2006 looked very much like the corona of November 1994, not the dipolar corona of early 1996, during the last minimum. As the onset of a new cycle occurs ~ 1 year after the minimum, both of these observations are consistent with the next solar cycle onset being delayed until late 2007 or early 2008.

3.8 *Can the sequence of observed solar cycle peaks be simulated and predicted?*

The first truly dynamo-based simulation of the sequence of peaks of past solar cycles and a forecast of solar cycle 24 was published by Dikpati & colleagues (Dikpati *et al.* 2006; Dikpati & Gilman 2006). These simulations and forecast were done by starting from the calibrated flux transport dynamo of Dikpati *et al.* (2004) and making certain modifications. First, in equation (1) for the poloidal field in terms of vector potential A, the link between the toroidal field in the dynamo at the bottom and the poloidal field at the surface is replaced by a surface forcing term that is derived from the waxing and waning of the observed poloidal fields created by the decay of tilted bipolar active regions in previous solar cycles. This represents a form of 2D (time-latitude) data assimilation in the model, a very common practice for meteorological forecast models, but perhaps the first time it has been used in a solar forecasting problem.

As a result of the above modification, no quenching of the Babcock-Leighton poloidal source, and no buoyancy mechanism are included in the model. However, the nonlinear quenching in the α-effect near the base of the convection zone is retained. Since this α-effect is much smaller compared to the Babcock-Leighton surface α-effect, in effect the model is mathematically changed from being a self-contained nonlinear system to a primarily linear system that is forced at the upper boundary by a measure of the Sun's past surface fields. The resulting equation for A is given by

$$\frac{\partial A}{\partial t} + \frac{1}{r\sin\theta}(\mathbf{u}\cdot\nabla)(r\sin\theta A) = \eta\left(\nabla^2 - \frac{1}{r^2\sin^2\theta}\right)A + \mathcal{F}(r,\theta,t) + \frac{\alpha B_\phi}{1+(B_\phi/B_0)^2}, \tag{3}$$

in which B_0 is the quenching field strength, set to 30 kGauss.

In this class of models, primarily the meridional flow speed determines the cycle period. However, we do not have observations of the time variation of this flow prior to 1996. So, in our initial approach, we estimate an average amplitude of meridional flow from the average period (10.75 yrs) of as many past cycles as we have high quality sunspot data for, which takes us back to cycle 12. If we use a meridional flow amplitude determined in this way, but force the model with data that has the observed period of each sunspot cycle, a phase mismatch in the link between the toroidal and poloidal fields grows to an unacceptably large value over several cycles' time integration. This makes simulation and forecast of cycle peaks impossible. To avoid this problem, Dikpati, deToma and Gilman stretched and compressed in time the observed data so that each cycle in the surface forcing had the same period, 10.75 years, as the intrinsic period of the dynamo, to avoid destructive phase mismatches. Thus this forecast model can predict amplitude, but not length simultaneously. A more sophisticated approach might involve an ensemble of 12 cycle simulations with different or time-varying meridional circulation, but that remains for the future.

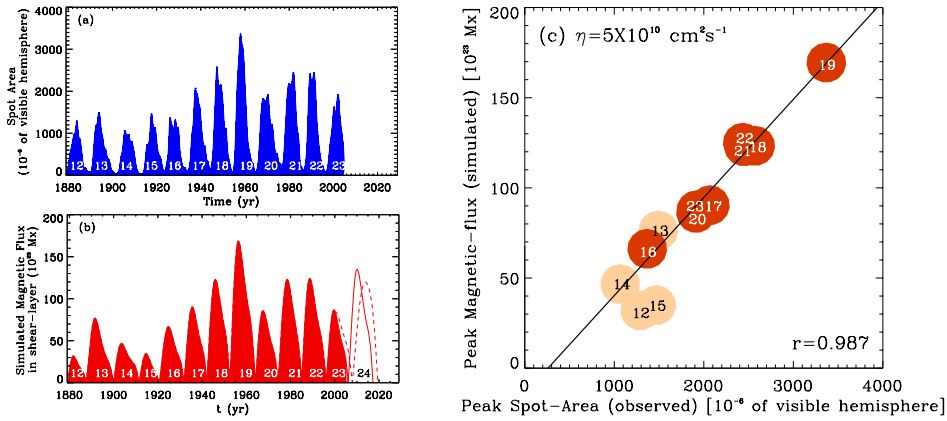

Figure 4. **(a)** Observed sunspot area data for cycles 12–23; **(b)** integral from 0–45° latitude of simulated toroidal magnetic flux in bottom shear layer for cycles 12–24, plus two forecasts for cycle 24; **(c)** scatterplot of sunspot area peaks vs. peak of toroidal magnetic flux integral.

Starting from a fully converged calibrated model solution, we initialized the model from the beginning of solar cycle 12, and ran it for the next 13 cycles extending through the upcoming cycle 24. The results of our simulations and predictions for the peaks of cycles 12–24 are shown in Figs. 4(a) and (b), adapted from Dikpati *et al.* (2006). Comparing the observed solar cycles with the sequence of simulated peaks in Fig. 4(a), we see that they are in good agreement, particularly beyond cycle 15 – the first few cycles the model needs to load its conveyor belt and to create its memory about the past cycles. The solid curve represents the case with meridional circulation fixed at a value that produces the 10.75 years dynamo period; it shows cycle 24 should have a $\sim$ 50% higher peak than cycle 23. The dashed curve represents a simulation that takes account of time variations in observed meridional circulation since 1996, as described above in section 3.7. For this case, cycle 24 is forecast to be $\sim$ 30% higher than cycle 23. There are many other forecasts for cycle 24, most saying it will be larger than 23, but some saying it will be smaller. Our forecast is the very first one made using a dynamo model with real solar data. The high skill of our forecast model is demonstrated in Fig. 3(b), which plots the observed peaks for cycles 12–23 against the peaks of the simulated toroidal flux in the overshoot tachocline between the equator and 45°. How the model achieves its forecast skill is discussed in detail in Dikpati and Gilman (2006). A key element is shown in Fig. 5 which plots the latitudinal poloidal field and the toroidal field at similar phases in cycles 19 and 20. It is the latitudinal fields from past 3 cycles, lined-up in the conveyor belt, that combine to form the seed for the next sunspot cycle's spot-producing flux, in contrast to the polar fields from last minimum.

3.9 *Criticisms and future calculations*

Certain criticisms have been put forward concerning forecasting solar cycle peaks using flux-transport dynamo models by Tobias, Hughes and Weiss. The authors of this letter state *a priori* that because they contain parameterizations, flux-transport dynamos have no predictive power. But all weather and climate forecasting models

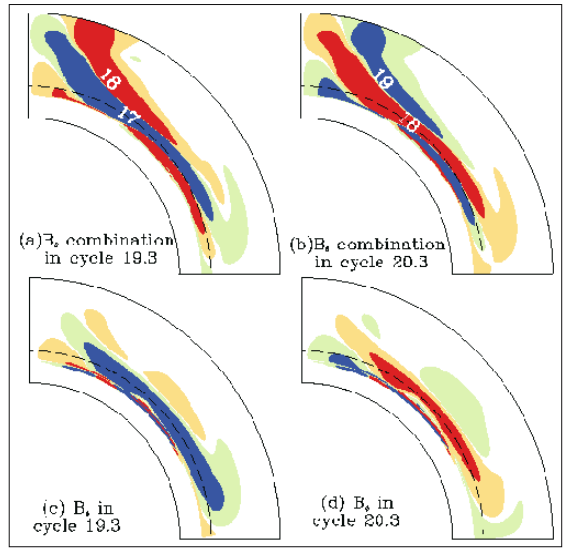

Figure 5. **(a, b)** Latitudinal component of simulated poloidal field (red and blue opposite signs) at phase 0.3 of cycles 19 and 20; **(c, d)** same for simulated toroidal field.

also have many parameterizations, and they have long been demonstrated to have skill. It is a logical certainty that predictive skill of ALL models, not just flux transport dynamos, can only be judged *a posteriori* by the results they produce. Also the skill of any model cannot be tested by using some other model with other physics, such as one that omits meridional circulation or time-latitude data assimilation. Much of the uncertainty of the effect of poorly known parameterizations of physical processes is removed by calibrating the model to solar observations, and then forecasting only departures from the calibrated solutions. This is a common and successful practice for forecast models in other fields, such as meteorology.

Tobias, Hughes and Weiss also claim that since the dynamo equations are extremely nonlinear, chaos intrinsic to the system makes prediction much more difficult, particularly for longer time periods. Within a solar cycle, there are short-term turbulent features which are probably governed by a variety of nonlinear processes including the buoyant rise of initially toroidal flux tubes. But we are not attempting to forecast them with our forced linear predictive tool. Obviously there are aggregate effects of many short-term nonlinear events which lead to, for example, the average surface poloidal fields that have a well-defined observed pattern. Our predictive tool captures this pattern. By analogy, mean flow in a river can be forecast without forecasting accurately the various eddies that occur in the flow.

Many additional calculations can and should be done with our solar cycle prediction model to test its robustness with respect to changes and fluctuations with time and space in various parameters currently included in it, such as the meridional circulation, turbulent magnetic diffusivity, α-effects, as well as the form and time dependence of the surface magnetic data from previous cycles. Such tests probably would be best done by employing so-called 'ensemble-forecast' methods, such as described in a meteorological context by Kalnay (2003), as well as more sophisticated methods

of assimilating observed data and iterating with updated forecast models, such as described in Kalnay (2003) and Talagrand (1997).

4. Concluding remarks

We have shown above that flux-transport dynamos when applied to the Sun can answer many important questions, from what determines the dynamo period to how the fields of previous cycles determine the amplitude of the next one. We plan many sensitivity tests of the model, and expect to generalize it, by using sequential data assimilation techniques to ultimately forecast period, amplitude and shape of a cycle. We already know that when we split the observed surface magnetic data into north and south hemispheres, we are able to correctly simulate the large differences in amplitude between hemispheres in later cycles when they occur.

Acknowledgements

This work is partially supported by NASA grants NNH05AB521, NNH06AD51I and the NCAR Director's opportunity fund. National Center for Atmospheric Research is sponsored by the National Science Foundation.

References

Babcock, H. W. 1961, *Astrophys. J.*, **133**, 572.
Basu, S., Antia, H. M. 2003, *Astrophys. J.*, **585**, 553.
Cowling, T. G. 1945, *MNRAS*, **105**, 166.
Dikpati, M. 1996, Thesis, Indian Institute of Science, Bangalore.
Dikpati, M., Charbonneau, P. 1999, *Astrophys. J.*, **518**, 508.
Dikpati, M., Gilman, P. A. 2001, *Astrophys. J.*, **559**, 428.
Dikpati, M., de Toma, G., Gilman, P. A., Arge, C. N., White, O. R. 2004, *Astrophys. J.*, **601**, 1136.
Dikpati, M., 2004a, Proceedings of SOHO14/GONG2004 Workshop (ESA SP-559), 233.
Dikpati, M., 2004b, *ASP Conf. Ser.*, **325**, 37 Workshop (ESA SP-559), 233.
Dikpati, M., Gilman, P. A., MacGregor, K. B. 2005, *Astrophys. J.*, **631**, 647.
Dikpati, M., Gilman, P. A., MacGregor, K. B. 2006, *Astrophys. J.*, **638**, 564.
Dikpati, M., de Toma, G., Gilman, P. A. 2006, *Geophys. Res. Lett.*, **33**, L05102.
Dikpati, M., Gilman, P. A. 2006, *Astrophys. J.*, **649**, 498.
Dikpati, M., Gilman, P. A. 2007, *Solar Phys.*, **241**, 1.
Dikpati, M., de Toma, G., Gilman, P. A., Arge, C. N., White, O. R. 2004, *ApJ*, **601**, 1136.
Garaud, P. 1999, *MNRAS*, **304**, 583.
Haber *et al.* 2002, *Astrophys. J.*, **570**, 855.
Kalnay, E. 2003, "Atmos. modeling, Data assimilation and Predictability", (Cambridge University Press).
Mestel, L., Weiss, N. O. 1987, *MNRAS*, **226**, 123.
Parker, E. N. 1955, *Astrophys. J.*, **122**, 293.
Parker, E. N. 1981, *Geophys. Astrophys. F. Mech.*, **18**, 175.
Parker, E. N. 1993, *Astrophys. J.*, **408**, 707.
Schüssler, M. 1975, *Astron. Astrophys.*, **38**, 263.
Stix, M. 1973, *Astron. Astrophys.*, **24**, 275.
Talagrand, O. 1997, *J. Met. Soc. Japan*, **75**, 1B, 191.
Wang, Y.-M., Sheeley, N. R. Jr. 1991, *Astrophys. J.*, **375**, 761.
Wang, Y.-M., Nash, A., Sheeley, N. R. Jr. 1989, *Astrophys. J.*, **347**, 529.
Wrubel, M. H. 1952, *Astrophys. J.*, **116**, 291.